Radiation Damage in Carbon Nanotubes: What Is the Role of Electronic Effects?

K. Nordlund*

Accelerator Laboratory, P.O. Box 43
FIN-00014 University of Helsinki, Finland

Abstract

Since carbon nanotubes are unique materials with respect to a wide range of properties, it is of interest to pose the question whether radiation damage in this system can be well understood based on traditional defect production models. A review of recent experimental and theoretical work in the field indicates that while at least heavy ion and high-energy electron damage can be well described with established approaches, considerable uncertainty remains regarding at least the effects of low-energy electrons on the damage production.

Contents

1 Introduction **358**

2 Electron Irradiation Effects **360**

3 Nuclear Collision Effects **362**

4 Damage by Electronic Effects? **364**

5 Discussion and Conclusions **366**

Acknowledgements **367**

References **367**

* E-mail: kai.nordlund@helsinki.fi

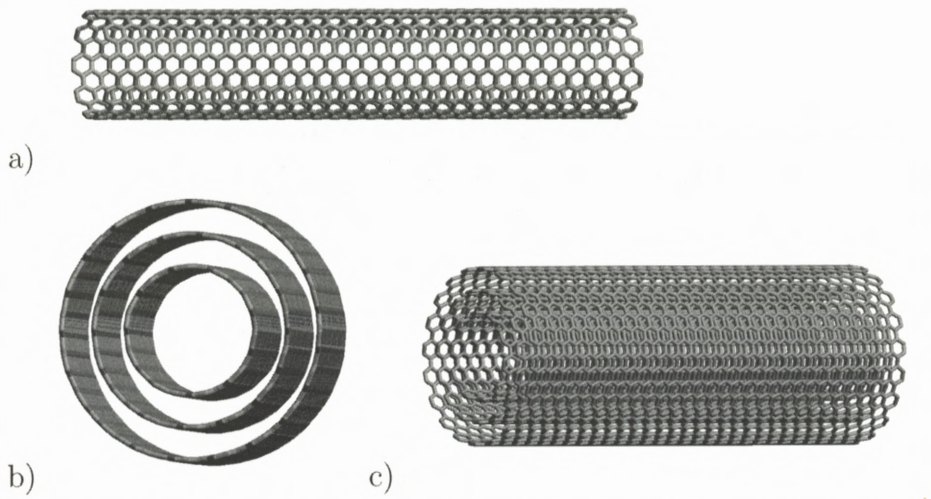

Figure 1. Atomic structure of carbon nanotubes, illustrated by plotting the chemical bonds joining the carbon atoms. (a) A single-wall carbon nanotube. (b) A triple-wall carbon nanotubes, almost axial view. (c) The same triple-wall carbon nanotube, viewed almost perpendicular to the axis.

1. Introduction

Notwithstanding the significant recent progress made in studies of radiation effects in carbon nanotubes, it remains unclear whether traditional radiation damage theories are fully applicable to describe irradiation effects in this prototypical nanosystem.

Carbon nanotubes are long, hollow cylinders of pure carbon consisting of either a single carbon cylinder or several concentric ones (Iijima, 1991; Ajayan and Iijima, 1992) (see Figure 1). The former kind are called single-walled nanotubes and the latter multi-walled ones. Their structure can conceptually be understood by imagining rolling up a single sheet of graphite ("graphene") into a cylinder with perfectly matching chemical bonds at the joining line (Dresselhaus et al., 2001), although it is noteworthy that the actual growth mechanism is very different (Raty et al., 2005). Despite being found already in the 1970s (Oberlin et al., 1976; Wiles and Abrahamson, 1978), large-scale interest in these systems emerged only in the 1990s (Iijima, 1991; Ajayan and Iijima, 1992; Iijima and Ichihashi, 1993). It quickly became clear that individual nanotubes have very interesting mechanical and electronic properties (Collins and Avouris, 2000; McEuen, 2000), giving rise to enormous basic and applied research interest (Baughman et al., 2002).

Studying irradiation effects in carbon nanotubes is well motivated both from a basic science and application point of view. On the basic science side, it is clear that the special geometry allows one to pose many interesting irradiation physics questions. From an applied science point of view, studies of radiation effects can be motivated in two ways. One can use irradiation as a way to introduce known controlled amounts of defects into a material, to understand damage effects on materials properties. This is quite important as even the best nanotubes manufactured to date do contain defects, and for instance electrical properties of nanotubes are highly sensitive to them (Fan et al., 2005; Gomez-Navarro et al., 2005). On the other hand, one can also look for ways in which irradiation can be used to modify nanotubes to obtain beneficial effects, such as tuning the electrical conductance of the tubes (Gomez-Navarro et al., 2005), using nanotubes as masks against ion irradiation (Yun et al., 2000; Krasheninnikov et al., 2002b), welding nanotubes together (Krasheninnikov et al., 2002a; Raghuveer et al., 2004) or introducing dopants into them (Kotakoski et al., 2005).

Central to both basic and applied science studies of irradiated carbon nanotubes is the understanding of the basic physics of damage production. This is a very interesting line of study for two reasons. First, the unique 1-dimensional nature and properties of nanotubes makes it questionable whether the traditional models of radiation effects are directly applicable to this system. Second, the nanotubes can be – and frequently are – studied one object at a time directly at the nanoscale. This makes it sometimes possible to study radiation effects experimentally down to the individual point defect level (Kimura-Hashimoto et al., 2004; Gomez-Navarro et al., 2005), something which has rarely been possible in any material. Thus studies of radiation effects in nanotubes might eventually lead to insights giving better understanding of radiation effects in other materials.

Since carbon nanotubes are either metallic or semiconductors with a relatively small band gap, the natural approach for attempting to understand radiation damage in them is using models developed for crystalline metals, semiconductors, and, of course, graphite. For these materials, the damage production can be understood in terms of three main classes of effects. For keV energy heavy ion irradiation, damage is dominated by nuclear collisions and cascades produced by them (Averback and Diaz de la Rubia, 1998; Smith, 1997). Electron irradiation can produce bulk damage only when the electron energy is high enough to produce atomic recoils with energies above the threshold displacement energy (Lucasson, 1975; Banhart, 1999). For MeV ions, when the electronic energy loss is of the order of 10 keV/nm or more, electronic effects can produce damage in some metals and semiconductors due to the high local heating around the ion track (Trautmann et al., 2000; Kanjijal, 2001; Bringa and Johnson, 2002).

During the last about eight years, a few groups have carried out systematic studies of electron and ion irradiation effects in nanotubes (for reviews, see Banhart, 1999; Krasheninnikov and Nordlund, 2004), and a great deal of understanding has been obtained. In this article, in the spirit of the Ion'06 workshop, the current understanding is summarized with an aim to explore where the damage production can clearly be treated with the conventional approaches, and where major open questions remain.

2. Electron Irradiation Effects

Electron irradiation of carbon nanosystems has been studied extensively by Banhart and co-workers with *in situ* experiments in electron microscopes. In these experiments, the electron beam of the microscope can be used to both irradiate and image the carbon nanosystems. These studies have shown that nanotubes can be damaged by electron irradiation. The irradiation has been shown to induce major structural rearrangements of the tubes, welding, and even phase transitions to the diamond phase (Wesolowski et al., 1997; Banhart, 1999, 2001; Terrones et al., 2000, 2002). As an example, the welding of two nanotubes is illustrated in Figure 2.

To establish how such effects have been understood, we first note that experiments have indicated that a threshold of damage production exists at an electron energy of about 86 keV (Smith and Luzzi, 2001). Assuming a direct knock-on between an electron and a carbon atom, this translates into a minimum threshold kinetic energy for damage production of 17 eV. This value is similar in magnitude to threshold energies found in conventional materials, including graphite (Nastasi et al., 1996; Andersen, 1979). Recoils produced by electron knock-ons above 86 keV will naturally lead to vacancy production, and indeed effects such as welding have been explained to be due to a high concentration of vacancies leading to coalescence of tubes (Terrones et al., 2000, 2002; Lopez et al., 2002; Jang et al., 2004) (cf. Figure 2).

One of the most dramatic irradiation effects known to occur in nanocarbon is the phase transition from graphene shells to diamond within carbon onions (concentric shells of fullerenes) (Wesolowski et al., 1997). This effect can also be understood based on vacancy and interstitial production: the irradiation-created vacancies in fullerenes and nanotubes have a special ability to recombine dangling bonds, leading to a shrinkage of the whole fullerene or nanotube (Sun et al., 2006). In the case of carbon onions, this leads to shrinkage of the concentric carbon spheres, with interstitials tending to migrate outwards due to the pressure gradient (Wesolowski et al., 1997; Banhart, 1999). This can

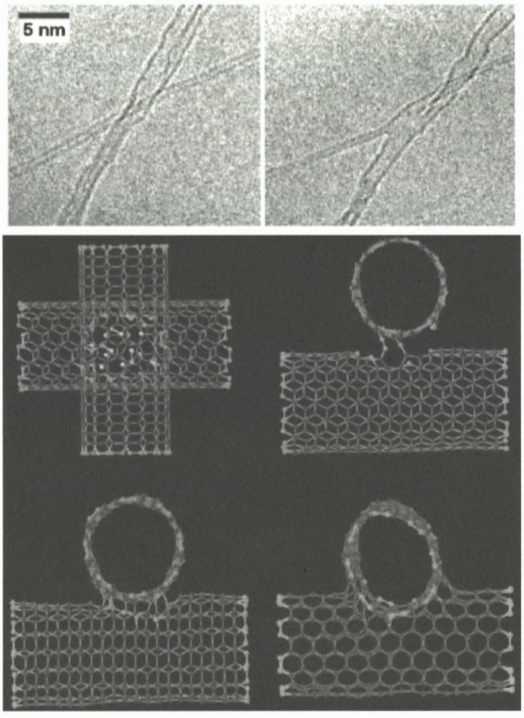

Figure 2. Welding of carbon nanotubes. The upper part shows an experimental TEM image of two crossed carbon nanotubes before and after electron irradiation. The two tubes were initially disjoint but then became welded by ion irradiation. The lower part shows a computer simulations of the welding process, based on creating vacancies in the near-junction region and allowing them to relax. Both figures are reprinted with permission from Terrones et al., 2002. Copyright (2002) by the American Physical Society.

lead to a high enough pressure to create diamond (Zaiser and Banhart, 1999; Astala et al., 2001).

Also the cross sections for recoil production by electrons have been considered in detail and found to be consistent with the observed damaging rates (Banhart, 1999). Thus it appears that the damage production in nanotubes by high-energy ($\gtrsim$ 100 keV) electron-irradiation can be understood well based on the traditional picture of knock-on displacements of atoms and subsequent defect migration.

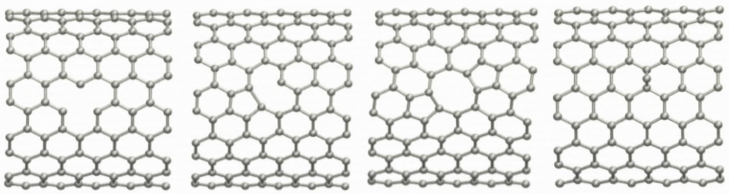

Figure 3. Some point defect structures in a carbon nanotube. (a) unreconstructed vacancy, (b) reconstructed "5-1db" vacancy, (c) divacancy, and (d) adatom on the outside of the tube.

3. Nuclear Collision Effects

The production of damage by low-energy ($\lesssim$100 keV) ion irradiation has been examined systematically with molecular dynamics (MD) simulations by Krasheninnikov and co-workers. These studies have shown that in single free-standing nanotubes ion irradiation produces predominantly single vacancies and small vacancy clusters (Krasheninnikov et al., 2001, 2002c). Some of these basic defects are illustrated in Figure 3. The initial vacancy structures produced during the irradiation by knocking out atoms are metastable: they contain dangling bonds, some of which tend to recombine to form more stable structures (Krasheninnikov and Nordlund, 2001; El-Barbary et al., 2003). Instead of becoming conventional interstitials (which would be atoms in the middle of a carbon hexagon in the tube) recoiled atoms either leave the tube or obtain an adatom-like structure. In this adatom-like structure a carbon atom is situated on a bond-centred site above or below the nanotube network (Nordlund et al., 1996). In a single tube this structure can be considered in many ways analogous to an interstitial.

In multi-walled tubes or a bundle of single-walled ones, also interstitials of a more conventional character exist in the form of carbon atoms lying between the individual carbon cylinders (Salonen et al., 2002; Pomoell et al., 2004). Sinnott and co-workers have shown that both low-energy electron and ion irradiation can be used to introduce such defects and thus cross-linking between the shells of multi-wall nanotubes (Pregler and Sinnott, 2006). For carbon peapods (fullerenes inside nanotubes) ion irradiation has somewhat similarly been shown to be able to cause cross-linking of the fullerenes (Hu et al., 2006).

The migration of the point defects has been examined with tight-binding and density-functional theory quantum mechanical simulations (Lehtinen et al., 2003; Krasheninnikov et al., 2004; Krasheninnikov et al., 2006). These studies show that the "adatom-interstitial" and vacancy exhibit rather special mobility properties: their mobility depends strongly on how the nanotube has been rolled up,

Figure 4. Example of a strongly damaged multi-wall carbon nanotube. The tube in the picture was irradiated by Ar ions with a range approximately half-way across the multi-wall tube, thus damaging the upper part strongly (Krasheninnikov et al., 2002b).

and on whether it is metallic or semiconducting. The interstitial is highly mobile, while the vacancy is less so. Once the vacancies have joined together to form di- or larger vacancy agglomerates, the mobility decreases strongly.

These theoretical results on migration are supported by recent transmission electron microscopy experiments (Kimura-Hashimoto et al., 2004) in which individual small immobile vacancy clusters produced by the electron irradiation were observed at room temperature. Since the irradiation was carried out just above the displacement threshold, the vacancy clusters must have formed by coalescence of single vacancies. Thus the experiment supports both the mobility of vacancies and immobility of larger clusters at room temperature.

The quantitative values of interstitial and vacancy mobility for the largest tubes studied are also in line with mobility values obtained in graphite (Thrower and Mayer, 1978), although some uncertainty exists in how these should be interpreted (El-Barbary et al., 2003).

We also consider whether the damage levels obtained are reasonable. In the MD simulations the damage builds up linearly with dose as no recombination occurs on the MD time scale, and amorphization occurs when most of the atoms have been displaced at least once. An example of a strongly damaged nanotube is shown in Figure 4. Even though some recombination does of course in reality always occurs due to long-time scale defect migration, recent kinetic Monte Carlo (KMC) simulations (Kotakoski et al., 2007) indicate that this effect becomes more important only at temperatures significantly above room temperature. At lower temperatures the formation of amorphous structures is not much slowed down by migration and recombination. Thus under the assumption that these MD and

KMC studies are correct, one may use simple displacement-per-atom (dpa) values obtained from binary collision approximation codes like TRIM/SRIM to examine whether reported amorphization fluences are reasonable.

Using the "vacancy" production numbers from SRIM-2003 (Ziegler, 2003), the dpa values of certain experiments on nanotube irradiation were estimated by the author of this Article. Unless the experimental papers reported a density of their material, a density of 0.5 g/cm^3 (typical of macroscopic nanotube materials like nanotube paper) was assumed. The threshold displacement energy was allowed to be at its default value for carbon. Since our aim is to make only order-of-magnitude estimates, such rough estimates are acceptable.

Raghuveer et al. (2004) reported major modifications of nanotubes by 10 keV Ga at a fluence of 10^{16} ions/cm^2. Using the SRIM calculations described in the previous paragraph, we obtained that this corresponds to a damage level of 8 dpa. Wang et al. (2004) showed clear transmission electron microscopy (TEM) images of nanotube amorphization after irradiation with 10^{17} ions/cm^2 50 keV C. This corresponds to a damage level of 6 dpa. Both values are quite reasonable, as at such high dpa values amorphization indeed would be expected, even accounting for some possible defect recombination.

4. Damage by Electronic Effects?

Summarising the discussion in the two previous sections, the basics of damage production by both electrons and ions in carbon nanotubes would appear to be well understood. However, considering some additional experiments makes this picture considerably less certain.

We first discuss proton irradiation of carbon nanotubes. Basiuk et al. (2002) irradiated carbon nanotubes with 3 MeV protons in air at room temperature, and subsequently analysed them in a TEM. They reported that at a fluence of 3×10^{16} ions/cm^2 this irradiation amorphized the tubes. Using a similar calculation as described in the previous section, this corresponds to a damage level of 0.0001 dpa. We checked that even accounting for Xe recoils or possible inaccuracies in the Xe or nanotube film thickness does not change this number by the several orders of magnitude needed to explain the amorphization by nuclear energy deposition.

Khare et al. (2003) irradiated a 0.5 μm single-wall nanotube film placed below a 16.75 μm Xe film at 15 K by 1 MeV protons. These samples were studied by Fourier transform infrared spectroscopy, Raman and TEM methods. The authors reported obtaining CH bonds and defects and changes in nanotube diameters, although quantitative damage levels were not reported. This irradiation, considering the Xe layer on top, corresponds to some 0.0001 dpa in the nanotube layer.

By contrast, Weaver and co-workers have carried out 2 MeV proton irradiation of nanotube paper and nanotubes in a polymer matrix (Weaver et al., 2004; Neupane et al., 2005) up to doses of 7×10^{16} ions/cm^2. They report on the one hand measurable resistivity and Raman spectroscopy effects already at a dose of 10^{12} ions/cm^2, but on the other hand interpret the results to mean that the tubes have a high radiation tolerance. Unfortunately the atomic structure of the samples after the irradiations is not characterised in these experiments.

The interpretation of these results is not straightforward. Since Khare does not report an overall damage level, it is of course possible that the damage level they observe is quite small, but it is not obvious how a damage level of only 0.0001 dpa could result in measurable changes in tube diameters. The amorphization reported by Basiuk et al. clearly cannot be explained by a damage level of 0.0001 dpa: this would be in contrast with the heavy ion dpa values discussed in the previous section by at least 4 orders of magnitude. This experiment was carried out in air, suggesting that oxidation or interaction with water may play a role on the results. However, even then it is difficult to understand why the tubes would amorphize: even though point defects created by the irradiation are likely to be oxygenated or hydrogen-stabilised, such defects have been observed at ambient conditions in other experiments without any reported runoff structural changes (Gomez-Navarro et al., 2005). If the effect is not explained by the presence of air, the only alternative explanation would be damage caused by electronic excitations. The electronic stopping by 1 MeV protons is some 2–3 orders of magnitude higher than the nuclear one, so plenty of electronic deposited energy would be available. It is again not obvious, however, what the mechanism could be. The nanotubes are metallic or semiconducting with a small band gap, and the electronic stopping is only some 0.05 keV/nm. Hence damage by electronic excitations of the kind associated with swift heavy ions would seem unlikely both by materials property and low stopping value (Kanjijal, 2001).

Although the effects of the TEM electrons with energies of $\sim$100 keV or more, can be well described by traditional ballistic knock-on mechanisms (cf. Section 2), there are some experimental indications that particles which can not possibly produce recoils above the 17 eV threshold can damage nanotubes. Yuzvinsky et al. (2005) reported that 5 keV electrons would cause major damage in nanotubes, and Miko et al. (2006) reported that ultraviolet light can affect electrical and mechanical properties of nanotubes. However, in both cases the effect was attributed to the presence of chemically active radicals from the environment. Skakalova et al. have shown that 1.3 MeV γ ion irradiation can be used to strengthen macroscopic nanotube materials. This effect could in principle be related to knock-on displacements of atoms by the highest-energy particles in an electron-gamma radiation

cascade, or to low-energy recoils produced by γ ray-nucleus collisions. It might also be related to production of radicals either in the surrounding atmosphere or impurities in the films.

5. Discussion and Conclusions

The literature overview presented in the previous sections has illustrated that the basic physics of keV heavy ion and hundreds-of-keV's electron irradiation damage in nanotubes appears to be fairly well understood. Although some unique features of the damage behaviour are observed in nanotubes, such as the chirality-dependent migration rates of point defects, the conventional theory frameworks appear to be well suited to understand the effects. However, considerable uncertainty exists on whether low-energy electronic excitations can cause damage in nanotubes.

The basic reason why it is natural to assume electronic excitations would not cause damage in nanotubes is that they are either metals or semiconductors with a small band gap. In bulk metals and semiconductors electronic stopping does not produce damage, except in the swift heavy ion regime where the electronic energy deposition is very large. Swift heavy ions are indeed known to produce damage and sputtering in graphite, but the energy depositions at which this is observed are much higher, of the order of 10 keV/nm (Liu et al., 1998; Tripathi et al., 2006), while for MeV protons it is of the order of 0.1 keV/nm, i.e. 2 orders of magnitude less.

Highly charged slow ions have been observed to produce electronic sputtering of carbon, but only for charge states larger than about +7 (Schulte and Holzapfel, 1997), which of course is not relevant for protons.

Although it is thus hard to understand how low-energy electron excitations could cause damage in nanotubes, there are several independent sets of experiments where nanotubes are damaged when the probability of producing knock-on recoils above the threshold must be very small or zero (cf. Section 4). All of these are, however, performed under conditions where the irradiated material is subject to the presence of air or other chemical compounds than nanotubes. Thus it is possible that the electronic excitations produce chemically active radical species around the nanotubes, which then react with the nanotubes. Hence at this stage it appears most likely that the low-energy electronic effects are not due to any unknown radiation physics, but rather to some interesting – and not well understood – radiation chemistry effects. Additional experimental and theoretical work will clearly be required to resolve the mechanisms involved.

Acknowledgements

The work giving the basis for the current discussion was funded by the Academy of Finland under the ELENA research project, and benefited from generous grants of computer time from CSC, the Finnish IT Center for Science.

References

Ajayan P.M. and Iijima S. (1992): Smallest carbon nanotube. Nature **358**, 23

Andersen H.H. (1979): The depth resolution of sputter profiling. Appl Phys **18**, 131

Astala R., Kaukonen M., Nieminen R.M., Jungnickel G. and Frauenheim T. (2001): Simulations of diamond nucleation in carbon-onion cores. Phys Rev B Rapid Commun **63**, 081402

Averback R.S. and Diaz de la Rubia T. (1998): Displacement damage in irradiated metals and semiconductors. In: Ehrenfest H. and Spaepen, F. (Eds), Solid State Physics, Vol. 51. Academic Press, New York, pp 281–402

Banhart F. (1999): Irradiation effects in carbon nanostructures. Rep Prog Phys **62**, 1181–1221

Banhart F. (2001): The formation of a connection between carbon nanotubes in an electron beam. Nano Letters **1**, 329–332

Basiuk V.A., Kobayashi K., Kaneko T., Negishi Y., Basiuk E.V. and Saniger-Blesa J.M. (2002): Irradiation of single-walled carbon nanotubes with high-energy protons. Nano Letters **2**, 789–791

Baughman R.H., Zakhidov A.A. and de Heer W.A. (2002): Carbon nanotubes – The route toward applications. Science **297**, 787

Bringa E.M. and Johnson R.E. (2002): Coulomb explosion and thermal spikes. Phys Rev Lett **88**, 165501

Collins P.G. and Avouris P. (2000): Nanotubes for electronics. Scientific American **283**, 62–69

Dresselhaus M.S., Dresselhaus G. and Avouris P. (Eds) (2001): Carbon Nanotubes, Synthesis, Structure, Properties and Applications. Springer, Berlin

El-Barbary A.A., Telling R.H., Ewels C.P., Heggie M.I. and Briddon P.R. (2003): Structure and energetics of the vacancy in graphite. Phys Rev B **68**, 144107

Fan Y., Goldsmith B.R. and Collins P.G. (2005): Identifying and counting point defects in carbon nanotubes. Nature Materials **4**, 906

Gomez-Navarro C., de Pablo P.J., J. Gomez-Herrero B.B., Garcia-Vidal F.J., Rubio A. and Flores F. (2005): Tuning the conductance of single-walled carbon nanotubes by ion irradiation in the Anderson localization regime. Nature Materials **4**, 534–539

Hu Y., Irving D.L. and Sinnott S.B. (2006): Ion deposition induced modification of carbon nanopeapods: A computational study. Chem Phys Lett **422**, 137

Iijima S. (1991): Helical microtubules of graphitic carbon. Nature **354**, 56–58

Iijima S. and Ichihashi T. (1993): Single-shell carbon nanotubes of 1-nm diameter. Nature **363**, 603

Jang I., Sinnott S.B., Danailov D. and Keblinski P. (2004): Molecular dynamics simulation study of carbon nanotube welding under electron beam irradiation. Nano Letters **4**, 109–114

Kanjijal D. (2001): Swift heavy ion-induced modification and track formation in materials. Current Science **80**, 1560

Khare B., Meyappan M., Moore M.H., Wilhite P., Imanaka H. and Chen B. (2003): Proton irradiation of carbon nanotubes. NanoLetters **3**, 643–646

Kimura-Hashimoto A., Suenaga K., Gloter A., Urita K. and Iijima S. (2004): Direct evidence for atomic defects in graphene layers. Nature **430**, 870–873

Kotakoski J., Krasheninnikov A.V., Ma Y., Foster A.S., Nordlund K. and Nieminen R.M. (2005): B and N implantation onto carbon nanotubes: Insight from atomistic simulations. Phys Rev B **71**, 205408

Kotakoski J., Krasheninnikov A.V. and Nordlund K. (2007): Kinetic Monte Carlo studies of defect mobility in carbon nanotubes. To be published

Krasheninnikov A.V. and Nordlund K. (2001): Stability of irradiation-induced point defects on walls of carbon nanotubes. J Vac Sci Techn B **20**, 728

Krasheninnikov A.V. and Nordlund K. (2004): Irradiation effects in carbon nanotubes. Nucl Instr Meth Phys Res B **216**, 355

Krasheninnikov A.V., Nordlund K., Sirviö M., Salonen E. and Keinonen J. (2001): Formation of ion-irradiation-induced atomic-scale defects on walls of carbon nanotubes. Phys Rev B **63**, 245405

Krasheninnikov A.V., Nordlund K., J.Keinonen and Banhart F. (2002a): Ion-irradiation induced welding of carbon nanotubes. Phys Rev B **66**, 245503

Krasheninnikov A.V., Nordlund K. and Keinonen J. (2002b): Carbon nanotubes as masks against ion irradiation: an insight from atomistic simulations. Appl Phys Lett **81**, 1101. Also selected to Virtual Journal of Nanoscale Science & Technology Vol. 6 Issue 7 (2002).

Krasheninnikov A.V., Nordlund K. and Keinonen J. (2002c): Production of defects in supported carbon nanotubes under ion irradiation. Phys Rev B **65**, 165423. Also selected to Virtual Journal of Nanoscale Science & Technology Vol. 5 Issue 16 (2002).

Krasheninnikov A.V., Nordlund K., Lehtinen P.O., Foster A.S., Ayuela A. and Nieminen R.M. (2004): Adsorption and migration of carbon adatoms on carbon nanotubes. Phys Rev B **69**, 073402

Krasheninnikov A.V., Lehtinen P.O., Foster A.S. and Nieminen R.M. (2006): Bending the rules: Contrasting vacancy energetics and migration in graphite and carbon nanotubes. Chem Phys Lett **418**, 132

Lehtinen P.O., Foster A.S., Ayuela A., Krasheninnikov A., Nordlund K. and Nieminen R.M. (2003): Magnetic properties and diffusion of adatoms on a graphene sheet. Phys Rev Lett **91**, 017202

Liu J., Hou M.D., Liu C.L., Wang Z.G., Jin Y.F., Zhai P.J., Feng S.L. and Zhang Y. (1998): Tracks of high energy heavy ions in HOPG studied with scanning tunneling microscopy. Nucl Instr Meth Phys Res B **146**, 356

Lopez M.J., Rubio A., Alonso J.A., Lefrant S., Metenier K. and Bonnamy S. (2002): Patching and tearing single-wall carbon nanotube ropes into multiwall carbon nanotubes. Phys Rev Lett **89**, 255501

Lucasson P. (1975): The production of Frenkel defects in metals. In: Robinson M.T. and Young Jr. F.N. (Eds), Fundamental Aspects of Radiation Damage in Metals. ORNL, Springfield, pp 42–65

McEuen P.L. (2000): Single-wall carbon nanotubes. Physics World **31**

Miko C., Milas M., Seo J.W., Gaal R., Kulik A. and Forro L. (2006): Effect of ultraviolet light irradiation on macroscopic single-walled carbon nanotube bundles. Appl Phys Lett **88**, 151905

Nastasi M., Mayer J. and Hirvonen J. (1996): Ion-Solid Interactions – Fundamentals and Applications. Cambridge University Press, Cambridge, Great Britain

Neupane P.P., Manasreh M.O., Weaver B.D., Landi B.J. and Raffaelle R.P. (2005): Proton irradiation effect on single-wall carbon nanotubes in a poly(3-octylthiophene) matrix. Appl Phys Lett **86**, 221908

Nordlund K., Keinonen J. and Mattila T. (1996): Formation of ion irradiation-induced small-scale defects on graphite surfaces. Phys Rev Lett **77**, 699

Oberlin A., Endo M. and Koyama T. (1976): Filamentous growth of carbon through benzene decomposition. J Cryst Growth **32**, 335

Pomoell J.A.V., Krasheninnikov A.V., Nordlund K. and Keinonen J. (2004): Ion ranges and irradiation-induced defects in multi-walled carbon nanotubes. J Appl Phys **96**, 2864

Pregler S.K. and Sinnott S.B. (2006): Molecular dynamics simulations of electron and ion beam irradiation of multiwalled carbon nanotubes: The effects on failure by inner tube sliding. Phys Rev B **73**, 224106

Raghuveer M.S., Ganesan P.G., D'Arcy-Gall J., Ramanath G., Marshall M. and Petrov I. (2004): Nanomachining carbon nanotubes with ion beams. Appl Phys Lett **84**, 4484

Raty J.Y., Gygi F. and Galli G. (2005): Growth of carbon nanotubes on metal nanoparticles: A microscopic mechanism from ab initio molecular dynamics simulations. Phys Rev Lett **95**, 096103

Salonen E., Krasheninnikov A. and Nordlund K. (2002): Ion-irradiation-induced defects in bundles of carbon nanotubes. Nucl Instr Meth Phys Res B **193**, 608–613

Schulte O. and Holzapfel W.B. (1997): Effect of pressure on atomic volume of Ga and Tl up to 68 Gpa. Phys Rev B **55**, 8122–8128

Smith B.W. and Luzzi D.E. (2001): Electron irradiation effects in single wall carbon nanotubes. J Appl Phys **90**, 3509

Smith R. (Ed.) (1997): Atomic & Ion Collisions in Solids and at Surfaces: Theory, Simulation and Applications. Cambridge University Prss, Cambridge, UK

Sun L., Banhart F., Krasheninnikov A.V., Rodriguez-Manzo J.A., Terrones M. and Ajayan P.M. (2006): Carbon nanotubes as high-pressure cylinders and nanoextruders. Science **312**, 1199

Terrones M., Terrones H., Banhart F., Charlier J.C. and Ajayan P.M. (2000): Coalescence of single-walled carbon nanotubes. Science **288**, 1226–1229

Terrones M., Banhart F., Grobert N., Charlier J.C., Terrones H. and Ajayan P.M. (2002): Molecular junctions by joining single-walled carbon nanotubes. Phys Rev Lett **89**, 075505

Thrower P.A. and Mayer R.M. (1978): Point defects and self-diffusion in graphite. Phys Stat Sol (a) **47**, 11

Trautmann C., Klaumünzer S. and Trinkaus H. (2000): Effect of stress on track formation in amorphous iron boron alloy: Ion tracks as elastic inclusion. Phys Rev Lett **85**, 3648

Tripathi A., Khan S.A., Kumar M., Baranwal V., Krishna R. and Pandey A.C. (2006): SHI induced surface modification studies of HOPG using STM. Nucl Instr Meth Phys Res B **244**, 225–229

Wang Z. et al. (2004): Amorphous molecular junctions produced by ion irradiation on carbon nanotubes. Phys Lett A **324**, 321–325

Weaver B.D., Landi B.J. and Raffaelle R. (2004): High radiation tolerance of carbon nanotube matrices for space power applications. In: Proceedings of the 2nd International Energy Conversion Engineering Conference, 16–19 August 2004, Providence, RI

Wesolowski P., Lyutovich Y., Banhart F., Carstanjen H.D. and Kronmüller H. (1997): Formation of diamond in carbon onions under MeV ion irradiation. Appl Phys Lett **71**, 1948–1950

Wiles P.G. and Abrahamson J. (1978): Carbon fibre layers on arc electrodes – I: Their properties and cool-down behaviour. Carbon **16**, 341

Yun W.S. et al. (2000): Fabrication of metal nanowire using carbon nanotube as a mask. J Vac Sci Technol A **18**, 1329

Yuzvinsky T.D., Fennimore A.M., Mickelson W., Esquivias C. and Zettl A. (2005): Precision cutting of nanotubes with a low-energy electron beam. Appl Phys Lett **86**, 053109. See also Erratum, Appl Phys Lett **87**, 069902 (E)

Zaiser M. and Banhart F. (1999): Radiation-induced transformation of graphite to diamond. Phys Rev B **79**, 3680

Ziegler J.F. (2003): SRIM-2003 software package, available online at `http://www.srim.org`

Index

This index has been compiled on the basis of keywords provided by the authors of individual contributions. Each entry refers to the start page(s) of the respective contribution(s).

adatoms 357
affinity level 465
affinity, electron 465
alkali layer 465
amorphisation 13, 227
amorphous materials 383
amorphous zones 329
amorphous-crystalline interfaces 227
amorphous-crystalline multilayers 227
analysis, ion beam 133
angular distribution 405
annealing, dynamic 227
approximation, Gaussian 151
athermal melting 293
atmospheres, generation of 13
atomic displacements 227
Auger electron spectroscopy 497
Auger electron spectroscopy, electronic temperatures 497
Auger electron spectroscopy, inner shell ionisation 497
Auger electron spectroscopy, track potential 497
band gaps, surface projected 625
Barkas correction 557
beam diagnostics 37
Bethe stopping theory 557
Betz–Grodzins models 595
binary encounter collisions 497
biological effectiveness 37
Bloch stopping theory 557
blocking 655
Bohr stopping theory 557
Bohr–Lindhard models 595
Bradley–Harper theory 207
bubbles 329
buried interfaces 133
carbon ions 357
carbon nanotubes 357
cells, ion tracks in 59
channeled particles, radiation from 655
channeling 731
channeling, energy loss in 655
charge exchange 557
charge state 109
charge transfer 625
charge transfer, multi-electron 625
charge transfer, resonant 625
chemical effects 357
Chudakov effect 699
classical *versus* quantal description 655
cluster emission 405, 433
cluster emission, fragmentation 405
cluster formation 405
cluster impact 433
collective excitations 497
configurational energy states 383
correction, Barkas 557
correction, shell 557
correlated emission 497
cosmic rays 13
Coulomb explosion 293
coupling, surface 497
craters 329, 433
crystal-glass transition 383

crystal-glass transition, amorphization 383
crystal-glass transition, ergodicity 383
crystal-glass transition, percolution transition 383
crystallisation, epitaxial 227
damage, electron irradiation 357
damage, ion 227
damage, lower-energy electron 357
damage, nuclear collision 357
damage, radiation 357, 731
dechanneling 655
defects, extended 329
defects, ion-induced 207
defects, point 357
density correction in stopping 557
deposition 87
deposition, radial energy 59
depth resolution, ultimate 133
detector, solid state 731
diagnostics, beam 37
diffusion, radiation enhanced 13
diffusion, surface 207
displacements, atomic 227
distribution, angular 405
distribution, energy 405
divertor 87
dosimetry 37
double strand breaks 59
dynamic annealing 227
dynamic screening 151
effects, chemical 357
effects, finite size 625
effects, relativistic 655
effects, single ion 329
effects, strong field 699
electron affinity 465
electron emission 525
electron emission, kinetic electron emission 525
electron emission, potential electron emission 525
electron irradiation damage 357
electron number statistics, coincident measurement 525
electron number statistics, surface-scattered projectiles 525
electron spectra 557
electron sputtering 357
electron yield, total 525
electronic desorption 13
electronic excitations 13
electron-photon coupling 263
emission, cluster 433
encounter collisions, binary 497
energy distribution 405
energy loss in channeling 655
energy states, configurational 383
energy, fusion 87
energy-loss profile, width of 151
energy-loss spectra 557
enhanced FIBs, need for 133
epitaxial crystallisation 227
epitaxy, solid phase 227
equilibrium charge states of ions in solids 595
erosion 87
evolution, morphology 187
evolution, nanophore 187
excitations, collective 497
excitations, electronic 13
experimental distinction between kinetic and potential electron emission 525
extended defects 329
FAIR project 109
fast melting 109
fast neutron recoil atoms 731
Fermi shuttle 497
finite size effects 625
formation length 699
fragmentation 699
free-electron metals *versus* band structure 625
fullerenes 357
fusion energy 87
fusion, inertial 109
gas release 731
gas trapping 731
Gaussian approximation 151
generation of atmospheres 13
grain sputtering 13
graphene 357
graphite 357
grazing incidence 525
guided self-organization, nanoscale morphology control 187

heating and cooling 655
heavy ions 595
high charges, primary ionisation 497
high-resolution 329
history 731
image potential 465
impact parameter dependence 151
impact, cluster 433
impurities and defects 655
inertial fusion 109
infinite velocity 465
instability 207
instability, morphological 187
insulator surfaces 525
insulators 595
insulators, amorphisable 263
insulators, non-amorphisable 263
interaction, plasma-surface 87
interfaces, amorphous-crystalline 227
interfaces, buried 133
internal and exit charge states 595
interstellar medium 13
interstitials 357
ion beam analysis 133
ion channeling 227
ion damage 227
ion emission, secondary 465
ion range in tissue 37
ion ranges 731
ion scattering limits 133
ion tracks 13
ion tracks, in cells 59
ionic crystals 263
ion-induced defects 207
ionisation potential 465
ionisation probability 465
ionization and excitation probability 405
ionization energy loss 699
ionization, multiple 151
ions carbon 357
ions, w-values for 37
irradiation, single cell 59
isotope separator 731
kinetic Monte Carlo 207
kinetics, relaxation 187
layer, alkali 465
level width 465
light ions 595
Lindhard theory 655
linear cascade sputtering 405
localised *versus* delocalised capture 625
low-energy electron damage 357
LPM effect 699
magnetospheric ions 13
materials, amorphous 11
measurements, stopping 557
melting, athermal 293
metal *versus* insulator surfaces 625
metal surfaces 525
metals 329, 595
micro beam 59
micrometeorite impact 13
microscopy, transmission electron 329
minimum yields and widths 655
monolayer resolution 151
morphological instability 187
morphology evolution 187
morphology, surface 207
multi-electron charge transfer 625
multilayers, amorphous-crystalline 227
multiple ionization 151
nanophore evolution 187
nano-structures 133
nanotubes, carbon, 357
need for enhanced FIBs 133
non-adiabatic transitions 625
non-proportionality effects, slow molecular projectiles 525
nuclear collision damage 357
nuclear lifetimes 655
nuclear spectroscopy 731
organic and molecular solids, desorption mechanism 405
organic and molecular solids, secondary ion formation 405
organic and molecular solids, sputter depth profile 405
parallel velocity effect 625
pattern formation 207
perturbation, strong 497
phase transition 109, 357
planetary regolith 13

planning, treatment 37
plasma-surface interaction 87
point defects 357
polyatomic projectile impact, emission mechanism 405
polyatomic projectile impact, excitation and ionization phenomena 405
polyatomic projectile impact, linear cascade and spike regime 405
probability, ionisation 465
proton pick-up 699
quantum dots 133
radial energy deposition 59
radiation chemistry 13
radiation damage 357, 731
radiation enhanced diffusion 13
radiation from channeled particles 655
radiation synthesis 13
radiological weight factor 59
radiolysis 13
radiotherapy 37
rate equation 625
recoil atoms, fast neutron 731
relativistic effects 655
relativistic effects, in stopping 557
relaxation kinetics 187
release, gas 731
resolution, monolayer 151
resonant charge transfer 625
ripples, 207
saturation effects 595
scattering 557
scattering limits, ion 133
screening 557
screening, dynamic 151
secondary ion emission 465
segregation 13
semiconductors 329, 595
sensitivity, ultimate 133
shell correction 557
shock wave 293
single cell irradiation 59
single collision 151
single ion effects 329
single strand breaks 59
slow hydrogen in solids, bound states 595
slow hydrogen in solids, pions 595
slow hydrogen in solids, positive muons 595
slow hydrogen in solids, positrons 595
solid phase epitaxy 227
solid state detector 731
spatial resolution, ultimate 133
spectra, electron 557
spectra, energy-loss 557
spectroscopy, Auger electron 497
spectroscopy, nuclear 731
spikes 433
sputter yield 207
sputtering 13, 207, 433
sputtering, angular distribution 433
sputtering, depth of origin 433
sputtering, electron 357
sputtering, energy distribution 433
sputtering, grain
sputtering, linear cascade 405
sputtering, molecular and organic solids 433
sputtering, preferential sputtering 433
sputtering, yield 433
stellar shocks 13
stellar winds 13
stoichiometry determination, ultimate 133
stopping 557
stopping, density correlation in 557
stopping, relativistic effects in 557
stopping measurements 557
stopping power 109
stopping power, ratios 37
stopping power, threshold 293
stopping theory, Bethe 557
stopping theory, Bloch 557
stopping theory, Bohr 557
straggling 557
strand breaks, double 59
strand breaks, single 59
strong field effects 699
strong perturbation 497
structure, track 59
supertail 731
surface coupling 497
surface diffusion 207
surface morphology 207
surface perturbation 465

surface projected band gaps 625
surface ripples 207
surface structure triangulation 525
surface topography 433
surfaces, insulator 525
surfaces, metal 525
swift-ion tracks 433
thermal spike 293
thermal vibrations 655
thermodynamics 293
thermodynamics, supercooling 293
thermodynamics, superheating 293
threshold behaviour 525
threshold, stopping power 293
tissue, ion range in 37
total electron yield 525
track description 263
track description, Poisson law 263
track description, threshold of track formation 263
track description, track morphology 263
track description, velocity effect 263
track mechanics 293
track mechanics, hillock formation 293
track mechanics, ion hammering 293
track model 263
track model, electron-photon coupling 263
track model, energy deposition 263
track model, linear energy loss 263
track model, radial energy distribution 263
track model, sputtering 263
track model, transient thermal process 263
track structure 59
tracks, swift-ion 433
transitions, non-adiabatic 625
transitions, phase 109
transmission electron microscopy 329
transport theory 433, 497
trapping, gas 731
treatment planning 37
triangulation, surface structure 525
tunnelling 625
tunnelling model 465
ultimate depth resolution 133
ultimate sensitivity 133
ultimate spatial resolution 133
ultimate stoichiometry determination 133
vacancies 357
velocity effect 557
velocity effect, parallel 625
viscoleastic properties 383
voids 329
warm dense matter 109
weight factor, radiological 59
width of energy-loss profile 151
work function 465
w-values for ions 37
yields and widths, minimum 655
zones, amorphous 329